Cerebral Cortex, September 2017;27: 4492–4502

doi: 10.1093/cercor/bhw253
Advance Access Publication Date: 22 August 2016
Original Article

ORIGINAL ARTICLE

Data Quality Influences Observed Links Between Functional Connectivity and Behavior

Joshua S. Siegel[1], Anish Mitra[2], Timothy O. Laumann[1], Benjamin A. Seitzman[1], Marcus Raichle[1,2], Maurizio Corbetta[1,2,3,4], and Abraham Z. Snyder[1,2]

[1]Departments of Neurology, Washington University School of Medicine at Washington University, St. Louis, MO 63110, USA, [2]Mallinckrodt Institute of Radiology, Washington University School of Medicine at Washington University, St. Louis, MO 63110, USA, [3]Department of Neuroscience, Washington University School of Medicine at Washington University, St. Louis, MO 63110, USA, and [4]Department of Neuroscience at University of Padua, Padua 35122, Italy

Address correspondence to Joshua S. Siegel, Department of Neurology, Washington University School of Medicine, 4525 Scott Ave., Box 8111, St. Louis, MO 63110, USA. Email: jssiegel@wustl.edu

Shared senior authors (Corbetta Maurizio and Synder Abraham)

Abstract

A growing field of research explores links between behavioral measures and functional connectivity (FC) assessed using resting-state functional magnetic resonance imaging. Recent studies suggest that measurement of these relationships may be corrupted by head motion artifact. Using data from the Human Connectome Project (HCP), we find that a surprising number of behavioral, demographic, and physiological measures (23 of 122), including fluid intelligence, reading ability, weight, and psychiatric diagnostic scales, correlate with head motion. We demonstrate that "trait" (across-subject) and "state" (across-day, within-subject) effects of motion on FC are remarkably similar in HCP data, suggesting that state effects of motion could potentially mimic trait correlates of behavior. Thus, head motion is a likely source of systematic errors (bias) in the measurement of FC:behavior relationships. Next, we show that data cleaning strategies reduce the influence of head motion and substantially alter previously reported FC:behavior relationship. Our results suggest that spurious relationships mediated by head motion may be widespread in studies linking FC to behavior.

Key words: functional connectivity, head motion, IQ, movement, resting state

Introduction

The number of resting-state fMRI (R-fMRI) studies has grown exponentially over the last decade (Birn 2012; Snyder and Raichle 2012). A principle analytic approach in these studies is computation of the interregional correlation of spontaneous fluctuations in the blood oxygenation level dependent (BOLD) signal. This measure is referred to as functional connectivity (FC). Many FC studies assume that interindividual differences in the magnitude of observed correlations reflect a biologically meaningful difference in brain function. Accordingly, FC has been used to study a wide range of neurological and psychiatric diseases as well as differences in cognitive function across the healthy population (Barkhof et al. 2014; Fornito and Bullmore 2015).

Sources of Noise and Spurious Correlation

A major challenge in the interpretation of FC:behavior analyses is removal of artifact from the BOLD signal. Head motion

(frame-wise displacement; FD) has long been recognized as a source of artifact in task-based magnetic resonance imaging (Friston et al. 1996; Siegel et al. 2014). This problem is particularly severe in R-fMRI because head motion generates spatially structured artifact that systematically alters FC measurements in characteristic ways (Power et al. 2012; Satterthwaite et al. 2012; Van Dijk et al. 2012). An FC:behavior finding that has spanned many studies is that the young, the elderly, and populations affected by neurologic or psychiatric abnormalities often exhibit "underconnectivity" relative to healthy young adults, especially in the default mode network (Andrews-Hanna et al. 2007; Fair et al. 2007; van Eimeren et al. 2009; Dosenbach et al. 2010; Liu et al. 2014). These studies emphasize, in particular, reduced FC between the medial prefrontal cortex and posterior cingulate cortex. This is among the FC most altered (reduced) by head motion (Power et al. 2012). Subsequent studies controlling for motion artifact and motion differences between groups found that such results may be largely spurious (Deen and Pelphrey 2012; Power et al. 2012; Satterthwaite et al. 2012; Chai et al. 2013; Fair et al. 2013; Tyszka et al. 2014). Despite these cautionary findings, many studies continue to report FC:behavior relationships without adequate consideration of head motion.

Approaches to Remove Artifact

Numerous preprocessing and data cleaning approaches have been developed to reduce the impact of imaging artifact (e.g., Jo et al. 2010; Shirer et al. 2015). Compensation for head motion by realignment and time course regression of realignment estimates (and their temporal derivatives) are used nearly ubiquitously. Beyond this, the neuroimaging field has yet to reach a consensus regarding what approaches should be taken or how strictly to apply criteria for cleanup or exclusion of corrupted data. Commonly used approaches for cleaning data include multiple time course regression, frequency filtering to remove cardiovascular, respiratory, motion-induced artifacts, censoring of frames flagged based on head motion and/or signal spikes, exclusion of high-motion subjects, and regression of measurable covariates of no interest. A comparative analysis of many of these approaches is given in Power et al. (2015) . Partial correlation has also been proposed as an alternative approach for removing spurious shared variance in correlation analysis (Smith et al. 2011). More recently, the application of independent component analysis to identify and remove unwanted components of the BOLD signal has been proposed (Salimi-Khorshidi et al. 2014). The value of each of these approaches in the study of FC:behavior relationships remains incompletely understood.

FC:Behavior in the Human Connectome Project

The Human Connectome Project (HCP) offers an unprecedented opportunity to understand how FC relates to task-evoked BOLD responses, structural connectivity, behavior, and genetics in a large population of 1200 healthy young adults (Van Essen et al. 2013). Prior work using FC data from the HCP has reported FC:behavior relationships as regards fluid intelligence and life success (Finn et al. 2015; Smith et al. 2015). The HCP consortium recently released data from 500 subjects. In addition to minimal preprocessing, these R-fMRI data have undergone processing steps designed to remove artifact (HCP FIX-ICA denoising pipeline) with the intention of providing clean, ready-to-use data (Smith et al. 2013). However, the degree to which head motion influences observed FC:behavior relationships in these data has not been systematically evaluated.

Using data from the HCP 500 subject release, we first ask which behavioral, demographic, and physiological measures correlate with head motion across subjects. Next, we establish how head motion affects BOLD signal correlations, both intersubject ('trait' analysis) and intrasubject across scanning sessions (state analysis). The intrasubject approach enables modeling of the effects of head motion on FC while avoiding potential neurobiological differences between high and low movers. Next, using the example of fluid intelligence, we measure intersubject FC:behavior relationships. We then estimate the influence of head motion by measuring the similarity between intrasubject effects of head motion and observed FC:behavior relationship. Finally, we ask how additional data cleaning approaches (not included in the HCP FIX-ICA denoising pipeline) alter computed FC:behavior relationships by reducing the effects of head motion.

Materials and Methods

Resting-State fMRI Data

We downloaded resting-state fMRI (R-fMRI) data from the HCP Q3 release that had been run through the HCP FIX-ICA denoising pipeline (https://db.humanconnectome.org/; Data Access Point in Fig. 1). In total, this data set included 461 healthy adults (ages 22–35 years, 271 females) scanned on a 3T Siemens connectome-Skyra scanner (Uğurbil et al. 2013). R-fMRI was acquired with multiband echo-planar imaging at a temporal sampling rate of 0.72 s per volume and 2-mm isotropic voxels. Each subject contributed 4×15 -min runs of R-MRI data acquired in 2 phase-encoding directions on 2 separate days (rfMRI_REST1_RL, rfMRI_REST1_LR, rfMRI_REST2_RL, rfMRI_REST2_LR). To enable cross-subject registration and surface mapping, T1-weighted and T2-weighted structural images of (0.7 -mm isotropic voxels) were also acquired, and EPI susceptibility distortions were corrected using B-zero field mapping. The downloaded data had been minimally preprocessed as described in Smith et al. (2013) and Glasser et al. (2013). Subject 14 626 was a duplicate and therefore removed. Three subjects (124220, 147030, 151526) with average FD greater than 4 standard deviations (SDs) above the mean were also removed leaving 457 subjects.

R-fMRI data from the first 177 subjects were reconstructed using an HCP-specific pipeline that was later improved (internally by the HCP). The present principal results were obtained using only data reconstructed with the improved pipeline (284 subjects). All analyses were repeated using all 457 subjects; the obtained results are reported in the supplement.

R-fMRI Preprocessing

Preprocessing steps applied prior to download (Fig. 1, HCP Processing) included the following: 1) one step resample (motion realignment, field map, and gradient distortion correction, Montreal Neurological Institute atlas registration), 2) whole-brain mean 10 000 intensity normalization, 3) cortical ribbon-based volume to surface mapping with exclusion of noisy voxels, 4) resampling to atlas-registered 32k mesh, 5) 2 mm full-width at half-maximum geodesic surface smoothing. Finally, the data were run though the HCP FIX-ICA denoising pipeline. FIX (FMRIB's ICA-based X-noiseifier) is an automated IC-classifier designed to remove artifactual components from FC data (Salimi-Khorshidi et al. 2014). Briefly, the HCP FIX-ICA denoising pipeline begins with high-pass filtering

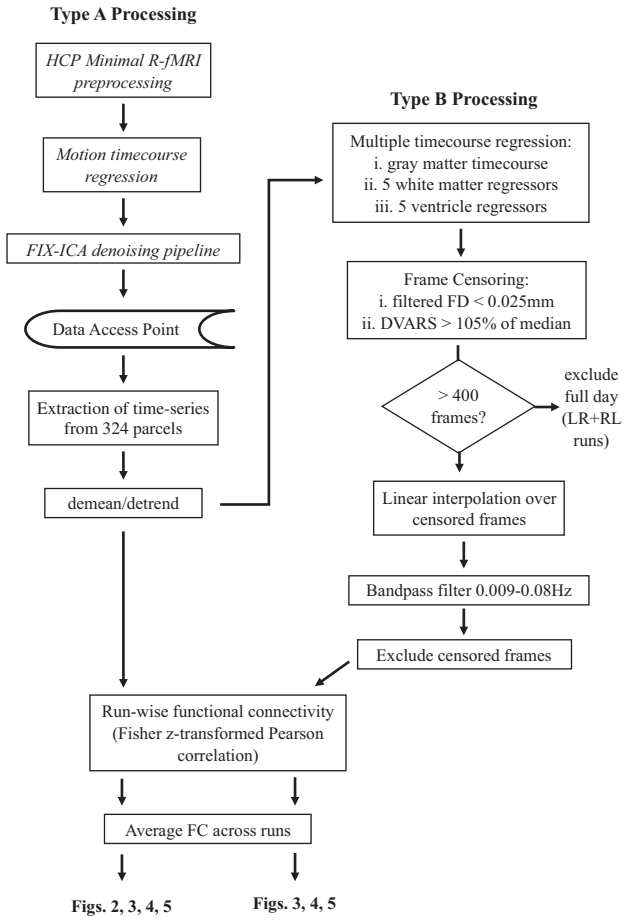

Figure 1. Data processing schematic. Boxes with black text indicate processing steps that occurred prior to accessing data. Surface projected and FIX-ICA pipelineR-fMRI data (e.g., rfMRI_REST1_LR_hp2000_clean.dtseries.nii) was accessed from https://db.humanconnectome.org. Italic text indicates processing steps implemented prior to access of R-fMRI data. Type B processing included a number of additional data cleaning steps implemented after parcel time series were extracted, demeaned, and detrended.

(cutoff = 1/2000 s) using fslmaths. Next, spatial ICA is used to deconstruct the data into constituent components. Components are then automatically classified as signal or noise based on spatial and temporal features. Finally, partial regression is performed using 24 motion regressors and all time courses from "noise" components. In additional analyses comparing data processing pipelines, HCP data not run through the FIX-ICA pipeline were additionally accessed from https://db.humanconnectome.org/.

Parcellation

Time series were extracted from a 324-region cortical parcellation (Gordon et al. 2016) (Supplementary Fig. S1). This parcellation is based on R-fMRI boundary mapping and achieves full cortical coverage and optimal within-region homogeneity. The original parcellation included 333 regions. Here, we excluded all regions with less than 20 vertices (ca. 50 mm^2). The final parcellation included 324 regions of interest (159 left hemisphere,165 right hemisphere). Subcortical regions were necessarily excluded as the parcellation technique operates in surface (2D) space, while subcortical data are volumetric (3D). Parcel time series were then demeaned, detrended, and variance normalized.

Type A FC Processing

In Type A processing (Fig. 1, left), data previously run though the HCP FIX pipeline were downloaded, parcellated, demeaned, and detrended. Pearson correlation coefficients were calculated between each parcel, and Fisher r-to-z transformed. Correlation values were calculated for each of the 4 runs and averaged to generate the connectivity matrix for each subject.

Type B FC Processing

Type B processing (Fig. 1, right) included all steps used in Type A processing followed by additional steps prior to calculating FC:

1. Multiple time course regression.
2. Bandpass filtering.
3. Frame censoring (scrubbing).
4. Run exclusion. If any run from either day contained less than 400/1200 frames postscrubbing (see below), then both the LR and RL runs from that day were excluded. Of note, 61/457 subjects had 1 day excluded, 32/457 subjects did not have any usable runs after scrubbing and were excluded entirely from further analysis. Below is a complete description of each step included in Type B processing.

Data Cleaning

Multiple Time Course Regression

Volume processed data were downloaded from the HCP for generation of tissue-based regressors. Regressors were calculated using white matter, ventricle, and gray matter masks. First, BOLD volumes were down-sampled to 3 mm^3 and tissue compartment masks were applied, excluding voxels not completely within the mask. Multiple tissue compartment regressors were generated by decomposition of white matter and ventricle time courses using PCA (Behzadi et al. 2007). Down-sampled voxel time courses were detrended prior to PCA and the first 5 eigenvectors were retained as regressor time courses. A single regressor was used for the average gray matter time course. Regressors were extracted from motion-corrected and intensity-normalized BOLD data passed through the FIX-ICA volume pipeline. Regressors were applied in a single step multiple time course regression (MTR). All frames were included in MTR.

Bandpass Filtering

Temporal frequency filtering was performed using a first-order Butterworth FIR filter with passband 0.009 to 0.08 Hz in the forward and reverse directions. Prior to filtering, time courses were padded with 1/0.009 or 112 frames on either end to prevent edge effects. When filtering was conducted in conjunction with scrubbing, censored frames were replaced using linear interpolation. This step insures that motion artifact in frames marked for removal do not blur into retained frames as a result of filtering (Carp, 2013).

Frame Censoring (Scrubbing)

Corrupted volumes were identified on the basis of FD as well as the voxel-wise differentiated signal variance (DVARS) (Smyser et al. 2010). FD indexes movement of the head from one volume to the next, and was computed as the sum of the absolute values of the differentiated rigid body realignment estimates at every time point with rotation evaluated at a radius of 50 mm.

The variance of differentiated signal (DVARS) indexes change in signal intensity from one volume to the next, and was calculated prior to nuisance regression as the spatial root mean square value of the temporally differentiated BOLD time series evaluated over the whole brain.

Pervasive high frequency noise in the FD traces was consistently observed across subjects. Spectral analysis (Fast Fourier Transform) revealed a peak in the power spectrum at 0.3 Hz (Supplementary Fig. S2), consistent with motion artifact attributable to respiration. Respiration is unlikely to reflect the same kind of head motion that introduces systematic artifacts into BOLD data (Power 2012, 2014); therefore, a 0.3 Hz low-pass filter was applied to the FD traces. A cutoff threshold of 0.025 mm was chosen after visual examination of the filtered FD traces to include normal variations in FD but exclude values suggestive of spikes in head motion (Supplementary Fig. S2). In some instances, DVARS spikes were observed without corresponding FD spikes (Supplementary Fig. S2, right). For this reason, a DVARS cutoff of 105% of the run median (since the DVARS baseline is run-specific) was used as an additional frame censoring criterion.

Additional Data Cleaning Approaches

In a final comparison between 8 data processing strategies, additional data cleaning approaches not included in Type B processing were implemented (Fig. 6). These include confound regression (at the population level), CompCor (multiple white matter and CSF regressors but no gray matter regressor), and partial correlation. See supplementary material for a full description of these approaches.

Behavioral Measures

The HCP data release includes 478 behavioral, demographic, and physiological measures. Descriptions of each measure can be found at wiki.humanconnectome.org/display/PublicData/HCP+Data+Dictionary+Public-+500+Subject+Release#HCPDataDictionaryPublic-500SubjectRelease. We selected a subset of 122 measures of potential neurobiological interest. Criteria for exclusion of measure included values missing for a majority of subjects, heavily skewed distribution, and likely irrelevance (e.g., "Is the subject born in Missouri?"). Retained measures included demographics (gender, income, education level, drug use, etc.), psychometrics (IQ, language performance, etc.), dia gnostic statistical manual (DSM) diagnoses (depression, antisocial personality disorder, etc.), personality traits such as "rule-breaking behavior, physiological" measures (blood pressure, body mass index [BMI], etc.), and brain size. Exclusion criteria and the complete list of retained measures are given in the supplementary material.

Relating Behavioral Measures to Head Motion

Average FD and DVARS values for each subject were compared with the 122 behavioral measures using Pearson correlation. Significance cutoffs were determined using permutation resampling (10 000 permutations; a cutoff was chosen for a familywise alpha of 0.05, that is, 5% of permutations showed one or more significant FD:behavior relationships).

Relating FC to Head Motion (IntraSubject)

The objective of the present work is to investigate the contribution of head motion to spurious FC:behavior relationships. However, intersubject correlations cannot distinguish between trait and state effects (e.g., real neurobiological differences that might exist between high and low movers versus artifacts that differentially accompany high versus low motion scans). Accordingly, data acquired over 2 days were used to disambiguate trait from state effects of head motion on BOLD signal correlations (Zeng et al. 2014). For each subject, both FC and FD were calculated on Days 1 and 2 and the cross-day difference in FC and FD was evaluated. Next, the cross-day FC-on-FD regression was computed to determine $\Delta FC/\Delta FD$ at every edge. The resulting matrix reflects intrasubject effects of head motion independent of trait differences.

Motion Influence on FC:Behavior

We define "motion influence" as the degree to which intrasubject FC:FD weights explain variance in intersubject FC:behavior relationships across ROI pairs (e.g., the Pearson correlation coefficient between intrasubject FC:FD and intersubject FC:behavior across all edges). Since motion effects are measured intrasubject and FC:behavior is measured across subjects, an observed correlation between them suggests that head motion likely contributes to observed FC:behavior relationships. Absent a repeated session design, state effects (e.g., direct effects of motion) would not be distinguishable from trait effects (i.e., subject-specific propensity to move). Thus, the fraction of variance in FC:behavior correlations explained by intrasubject FC:FD weights represents a more reliable estimate of motion influence. Results obtained using this approach are shown in Figures 3, 5, and 6.

Because FC correlations are nonindependent, statistical significance of motion influence on FC:behavior was assessed by permutation resampling. Specifically, covariance between intrasubject FC:FD weights and FC:behavior was compared with a null distribution using the following method. We simulated the null hypothesis (no influence of head motion on FC:IQ) by replacing IQ values with randomly permuted normally distributed values (IQ_{perm}). For 1000 such permutations, a single measurement of the covariance between FC:FD and FC:IQ_{perm} was recorded. A *P*-value (P_{perm}) was assigned for actual motion influence by determining how many out of 10 000 permutations showed a larger covariance. This same distribution of covariance values was used to assign a *P*-value to motion influence across the 19 behavior measures. However, 2 separate distributions were generated to test motion influence in Type A and Type B data.

Surface Projection

Matrix (324 × 324) results, generated by correlating FC matrices with other measures (FD or behavior) across subjects, were projected to brain surface regions (324 × 1) for visualization. Each matrix produced a positive and negative projection. In the positive projection, the value within each parcel is the mean of the top quartile of all of its connections (80/323). The negative projection is the mean of the bottom quartile. This approach was previously described by Smith et al. (2015). FC:IQ projection maps were thresholded at 0.135 based on a familywise false positive rate (alpha) of 0.05 (i.e., 5% chance of one or more brain parcels passing significance) over 10 000 permutations of IQ scores.

100-Subject Subgroup FC:Behavior Analysis

The percent of FC:behavior correlations with a significance of $P < 0.05$ (multiple comparisons uncorrected) was used as a descriptive statistic. By definition, 5% represents the number of

correlations expected by chance. To assess the sampling variability of this measure, multiple subgroups were created, each including 100 randomly selected (without replacement) subjects. For each subgroup, a Pearson correlation was computed between FC at every edge (324-choose-2 = 52 362 edges) and behavior. The distribution of the number of "significant" ($P < 0.05$) FC:behavior correlations was tabulated for each data processing regime.

Code Availability

The full matlab analysis script is freely available at www.nil.wustl.edu/labs/corbetta/resources/.

Results

Head Motion Correlates with Other Behaviors

Of the 478 behavioral, demographic, and physiological measures that accompany HCP data sets, 122 were selected as being of neurobiological interest prior to analyses. Of these 122 measures, 23 showed a significant correlation with head motion after familywise multiple comparison correction ($P_{uncorrected} < 0.00056$). These results are listed in Table 1. Behaviors negatively correlated with head motion index cognitive ability, e.g., reading engagement (subjects were asked to read and pronounce words and scored on accuracy), education level, and fluid intelligence (measured using the Penn Progressive Matrices). Measures positively correlated with head motion included psychiatric scales (DSM diagnoses and adult self-report [ASR] behavioral syndromes), tobacco use, and obesity (BMI, weight, blood pressure).

Table 1 Correlates of in-scanner head motion

Subject measures	Pearson *r*
ReadEng (AgeAdj)	−0.23
ReadEng (Unadj)	−0.23
Vocabulary (AgeAdj)	−0.19
Dexterity (Unadj)	−0.18
CardSort (Unadj)	−0.18
Dexterity (AgeAdj)	−0.18
CardSort (AgeAdj)	−0.18
Education	−0.17
Fluid intelligence	−0.17
Spatial orientation	−0.17
Vocabulary (unadjj)	−0.17
Emotion recognition	−0.16
DSM somatic problems (pct)	0.16
DSM antisocial (raw)	0.16
ASR externalizing (raw)	0.16
DSM somatic problems (raw)	0.16
Tobacco use 7 day	0.18
Diastolic blood pressure	0.18
ASR externalizing	0.18
Tobacco use today	0.2
Systolic blood pressure	0.23
Weight	0.52
Body mass index (BMI)	0.66

One hundred and twenty-two measures (behavioral, demographic, and physiological) were compared with average subject head motion. Significance thresholds were set at $P < 0.00056$ based on permutations. Twenty-three measures showed significant correlation. Pearson *r*-values are shown at right. Average FD and absolute change in FD between days were correlated at $r = 0.45$.

Twenty-two measures correlated with frame-to-frame signal variance (DVARS) with a *P*-value below the permutations cutoff (Table S1). Measures positively correlated with DVARS included negative personality scales (e.g., anger/aggression) as well as hematocrit, gender, brain volume, weight, and BMI. No negative correlations with DVARS were significant by permutation resampling.

Trait and State Effects of Head Motion on FC

Data acquired over 2 days were used to assess both intersubject (trait) and intrasubject across-day (state) effects of head motion on BOLD signal correlations. Type A processed FC data (see Methods and Fig. 1) showed a stereotypical topography of FC:motion correlations (Fig. 2). Pronounced FD-related increases in measured FC were observed between the DMN and task positive networks (black ovals in Fig. 2*a*/*b*). Conversely, head motion corresponds to reduced FC within the DMN (blue oval in Fig. 2*a*/*b* and negative weight projection in Fig. 2*c*). Importantly, trait effects of motion were very similar to state effects of motion (Pearson correlation of trait effect and state effect: $r = 0.643$, $P_{perm} < 0.0001$). In other words, the FC signature of increased propensity to move across subjects (trait) was very similar to the FC signature of variability in movement across sessions within an individual (state) (Power et al. 2012; Satterthwaite et al. 2012; Van Dijk et al. 2012). Taken together, these findings indicate that state characteristics associated with motion artifact potentially mimic other trait characteristics of other behaviors correlated with head motion in Table 1. This hypothesis was directly tested by developing an assay for motion influence on FC:behavior topography.

Head Motion Influences FC:Behavior Topography

To explore the influence of head motion on FC:behavior relationships, we compared intrasubject FC:FD to intersubject FC:behavior (see Methods: Motion Influence on FC:behavior). FC data analyzed with Type A processing were correlated with fluid intelligence (IQ; Penn progressive matrix score) and matrix results were projected onto the cortical surface (Fig. 3*a*). The value for each parcel is the mean of the top quartile of all of its connections; the map is thresholded at a familywise alpha of 0.05.

Across subjects, IQ correlates negatively with head motion (Table 1). Hence, we may expect to observe a negative correlation influence of head motion on FC:IQ. This result is shown on the right side of Figure 3*a*. Across all edges, FC:FD weights were negatively correlated with FC:IQ weights ($r = -0.31$, $r^2 = 0.10$, $P_{perm} = 0.0083$). Thus, motion influence explains roughly 10% of variance in the observed FC:IQ relationship. Note the similarity between negative weights in Figure 2c (i.e., connections that become weaker with head motion) and positive weights in Figure 3*a*. Since the influence of head motion was measured intrasubject and FC:IQ was measured across subjects, the observed relationship between FC:IQ and FC:FD is not simply attributable to an inherent correlation of IQ with head motion (Zeng et al. 2014).

An analysis parallel to that illustrated in Figure 3*a* was repeated for all 19 behavioral measures that showed a relationship with FD (Table 1). Four physiological measures (e.g., diastolic blood pressure) were excluded. Measures negatively correlated with head motion (IQ and other measures with a negative value in Table 1) were sign-inverted. FC:behavior weights then were averaged across the 19 measures. The

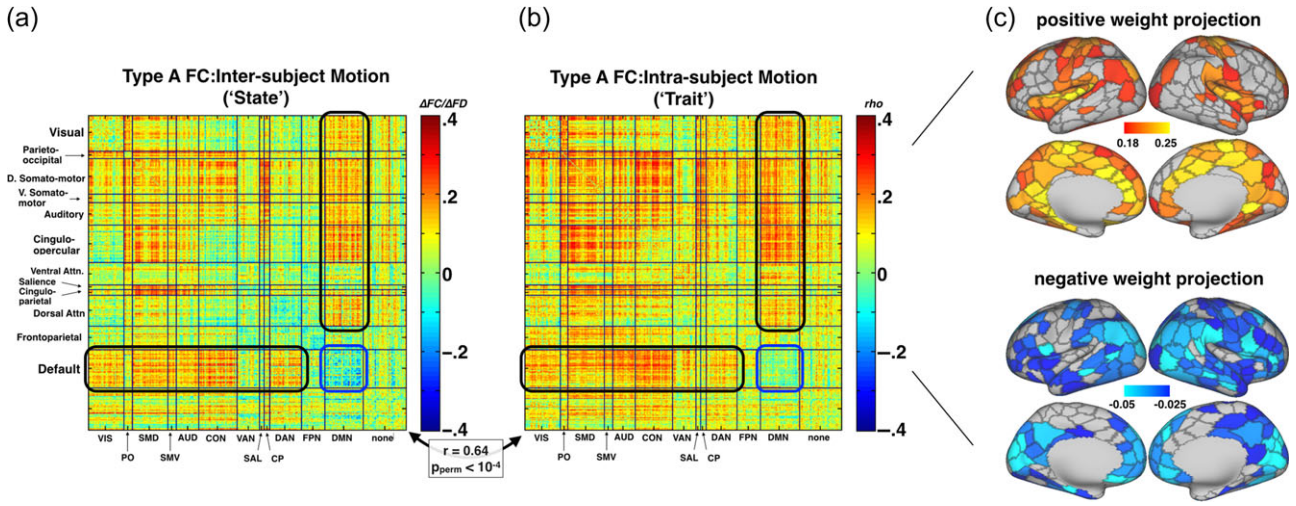

Figure 2. Head motion exerts a stereotyped influence on FC. (*a*) Full matrix of intersubject FC:FD correlation coefficients, measured with Type A processed FC data. (*b*) Full matrix of intrasubject (between day) FC:FD correlation coefficients. The spatial correlation between intrasubject and intersubject measures was $r = 0.64$. In (*c*) the top positive and negative intrasubject FC:FD weights are projected to parcels on the brain surface. The value for each parcel in the positive projection is the mean of the top quartile of values from all of its connections. The negative projection is the bottom quartile. RSN abbreviations: VIS = Visual network (38 ROIs); PO = parieto-occipital (7 ROIs); SMD = dorsal somato-motor (37 ROIs); SMV = ventral somato-motor (8 ROIs); AUD = auditory (23 ROIs); CON = cingulo-opercular (39 ROIs); VAN = ventral attention (23 ROIs); SAL = salience (4 ROIs); CP = Cingulo-parietal (5 ROIs); DAN = dorsal attention network (32 ROIs); FPN = frontoparietal control network (24 ROIs); DMN = default mode network (40 ROIs); NON = no assigned network (44 ROIs).

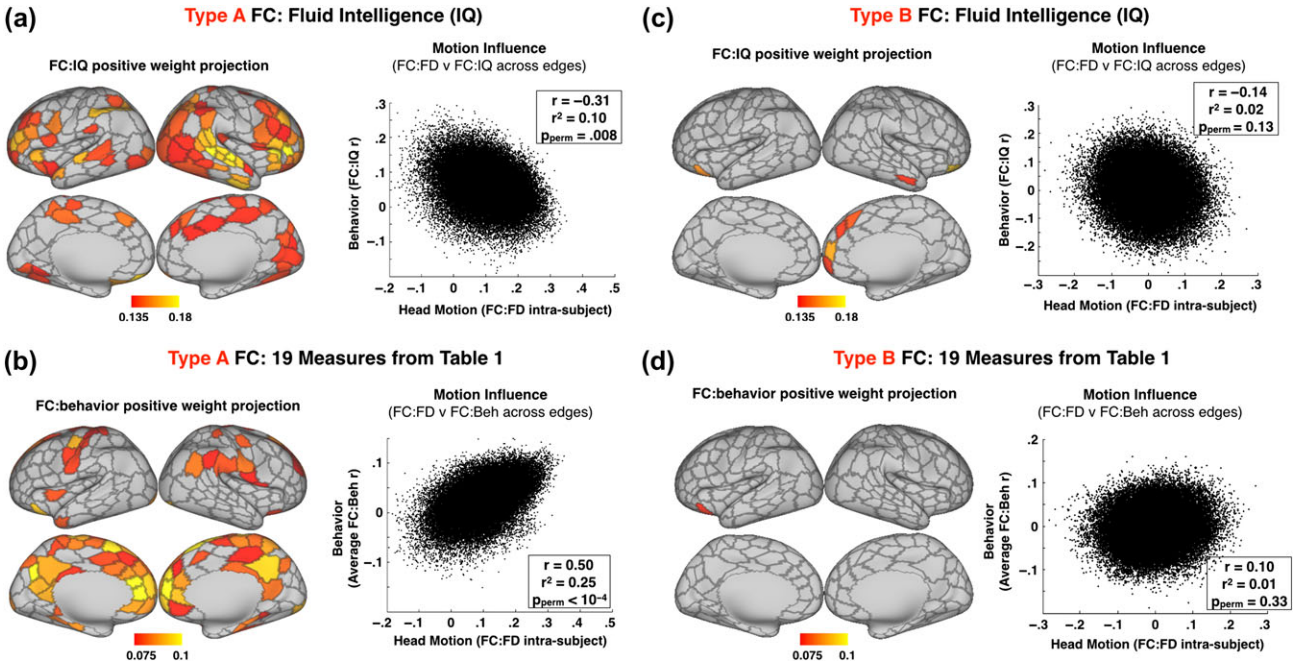

Figure 3. Motion influences FC:IQ topography. This influence decreases with Type B FC processing. Each scatter plot shows FC:FD (intrasubject) weights versus FC: behavior (intersubject) correlations. Each dot represents one of the 52 326 FC edges (324-choose-2). A larger correlation suggests greater head motion influence. P_{perm} denotes the *P*-value generated by permutations testing as described in the methods–motion influence on FC:behavior section. (*a*) Left: map of connection strength increases associated with IQ after Type A preprocessing (projection of top matrix weights). Right: scatter plot showing motion influence on Type A FC:IQ relationships. FC:IQ and FC:FD are correlated at $r = -0.31$, $r^2 = 0.10$, $P_{perm} = 0.008$. (*b*) Left: map of connection strength increases consistently associated with 19 motion-correlated behavioral measures in Table 1 (excluding 4 physiological measures, flipping negatively correlated measures). Weights are averaged across measures and then projected. Right: scatter plot showing motion influence on average FC:behavior relationships. FC:behavior and FC:FD are correlated $r = 0.50$, $r^2 = 0.25$, $P_{perm} < 0.0001$. Panels (*c*) and (*d*) were generated with identical methods to (*a*) and (*b*), but with Type B FC data instead of Type A.

results of this analysis (Fig. 3*b*) revealed a positive influence of head motion on FC:behavior relationships (opposite to that observed with IQ because of to sign inversion). FC:behavior weights were strongly correlated with FC:FD across edges ($r = 0.50$, $r^2 = 0.25$, $P_{perm} < 0.0001$) and showed similar topography (compare Figs. 2*c* and 3*b*).

We hypothesized that removal of artifactual variance in BOLD fMRI data would reduce the influence of head motion on

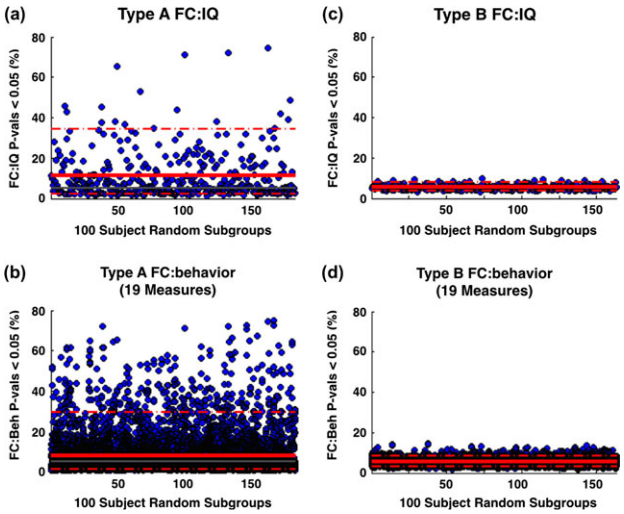

Figure 4. Comparing global FC-behavior relationships. Each blue dot represents the proportion of edges with FC:behavior correlation $P < 0.05$ for one 100-subject subgroup. The solid and dashed red lines represent mean and 95% bounds across subgroups, respectively. (*a*) For Type A subgroups, 11.4 ± 11.9% (mean ± SD) of edges correlated with IQ at $P < 0.05$ (uncorrected). (*c*) For Type B subgroups, 5.8 ± 1.2% of edges correlated with IQ at $P < 0.05$. (*b*/*d*) The same procedure is applied to all 19 motion-correlated measures. On average, for Type A and Type B subgroups, 7.9 ± 10.0 and 5.6 ± 1.5% of edges, respectively, correlated with behavior at $P < 0.05$.

FC:behavior correlations. Type B processing following Power et al. (2014; Fig. 1) was implemented to test this hypothesis. Type B processing resulted in a much more sparse topography of FC:IQ relationships (compare Fig. 3*a* vs. Fig. 3*c*). The influence of head motion on FC:IQ was no longer significant ($r = -0.14$, $r^2 = 0.02$, $P = 0.129$). Figure 3*d* illustrates the average FC:behavior relationship obtained from the 19 FD-correlated measures. Type B processing eliminated nearly all FC:behavior relations shown in Figure 3*b*. Full matrices for intrasubject FC:FD, intersubject FC:FD, FC:IQ and FC:behavior average for Type A and Type B FC data are shown in Figure S3. Note also that the magnitude of intrasubject motion effects, and the similarity between state and trait motion effects was much smaller with Type B processing ($r = 0.03$). These 2 observations suggest that spurious effects of motion are substantially reduced, but unique trait effects of motion may still be present. Figures 2 and 3 include only fMRI data obtained using reconstruction software version 2 (284 subjects). The analysis was repeated with all 457 subjects in the Q3 data release (Figure S4). Results were comparable although motion influence on FC:IQ is only trending toward significance ($r = -0.20$, $P_{perm} = 0.074$).

If imaging artifacts influence FC:behavior relationships, then better cleaning should reduce not only the prevalence of spurious relationships but also measurement variability. To test this hypothesis, we divided Type A and Type B processed FC data into random subgroups of 100 subjects each. For each subgroup, the number of significant FC:behavior correlations ($P < 0.05$) was used as a descriptive measure. Thus, 5% of correlations are expected to be significant by chance.

Figure 4*a* displays the percent of edges that showed FC:IQ relationship in 185 Type A subgroups. High variability was observed across subgroups. On average, 11.4 ± 11.9% (mean ± SD) of edges correlated with IQ at $P < 0.05$ (uncorrected). By contrast, following Type B processing, 5.8 ± 1.2% of edges correlated with IQ at $P < 0$ 0.05 (Fig. 4*c*). Note that the distribution of FC:IQ correlations across all edges (mean = 5.8%) was still significantly above the chance level of 5% (t-stat = 9.86, $P < 0.001$). Thus, 5.8% may be consistent with a real but spatially sparse FC:behavior relationship.

Figure 4*b*/*d* shows results parallel to Figure 4*a*/*c* for all 19 behavioral measures in Table 1. Following Type A processing, 7.9 ± 10.0% of edges correlated with behavior at $P < 0.05$. Following Type B processing, 5.6 ± 1.5% of edges correlated with behavior at $P < 0.05$ (Fig. 4*e*). Thus, Type B processing reduced the number of edges showing "significant" FC:behavior relationships and, importantly, substantially reduced variability across subgroups.

Type B Processing Consistently Reduced the Influence of Head Motion

Figure 3 demonstrates that FC:FD (intrasubject) and FC:behavior (intersubject) measures are correlated across edges. This observation implies that the topography of apparent FC:IQ correlations obtained with Type A processing is influenced by head motion (Fig. 3*a*). This relationship was substantially reduced by Type B processing (Fig. 3*c*).

Figure 5 shows results similarly comparing motion influence in Type A versus Type B processing across other behavioral measures. To facilitate visual comparison, the already-reported comparison of head motion influence on observed FC:IQ correlation is repeated in Figure 5*a*. Next, we generalized this analysis to other behavioral measures. First, we identified 4 measures not in Table 1 that showed a large motion influence following Type A FC processing. These measures were rule breaking, anger/aggression, life satisfaction, and amount of sleep (Fig. 5*b*). A large absolute correlation suggests that FC:behavior relationships are well explained by head motion; the sign of the correlation reflects the valence of the measure (i.e., rule breaking relates positively to head motion, whereas amount of sleep relates negatively to head motion). In all 4 cases, Type B processing substantially reduced the influence of head motion (Fig. 5*b*). Similar effects of Type B processing were observed across the 122 measures of potential neurobiological interest (Fig. 5*c*). The plotted values in Figure 5*c* are the r^2 values between FC:FD and FC:behavior in Type A versus Type B processing, as reported in Figure 5 *a*/*b*. The line of identity corresponds to equal motion influence in Type A and Type B data. Figure 5*c* indicates that Type B processing consistently reduced the degree to which head motion influences apparent FC:behavior relations.

Motion Influence in Different Data Cleaning Approaches

Several processing steps, some included in Type B and some not, have been proposed to reduce the influence of motion on FC analyses. We preprocessed FC data using 8 regimes and assessed motion influence in each (see supplementary material). These processing regimes variably included FIX-ICA pipeline, MTR, frame censoring, exclusion of high-motion subjects, and partial correlation (Fig. 6). For each regime, motion influence was calculated across the 19 (nonphysiological) measures from Table 1. Figure 6 reports the mean and standard error of motion influence on FC:behavior estimates for each processing regime. Type B processing showed significantly less motion influence than minimal preprocessing, Type A, scrubbing alone (Type A + scrub) or global signal regression with low-pass filtering ("Finn et al.") ($P < 0.05$, 2-tailed paired *t*-tests, Bonferroni corrected for 8 comparisons). However, "CompCor + scrub" and "Type A + partial correlation" also

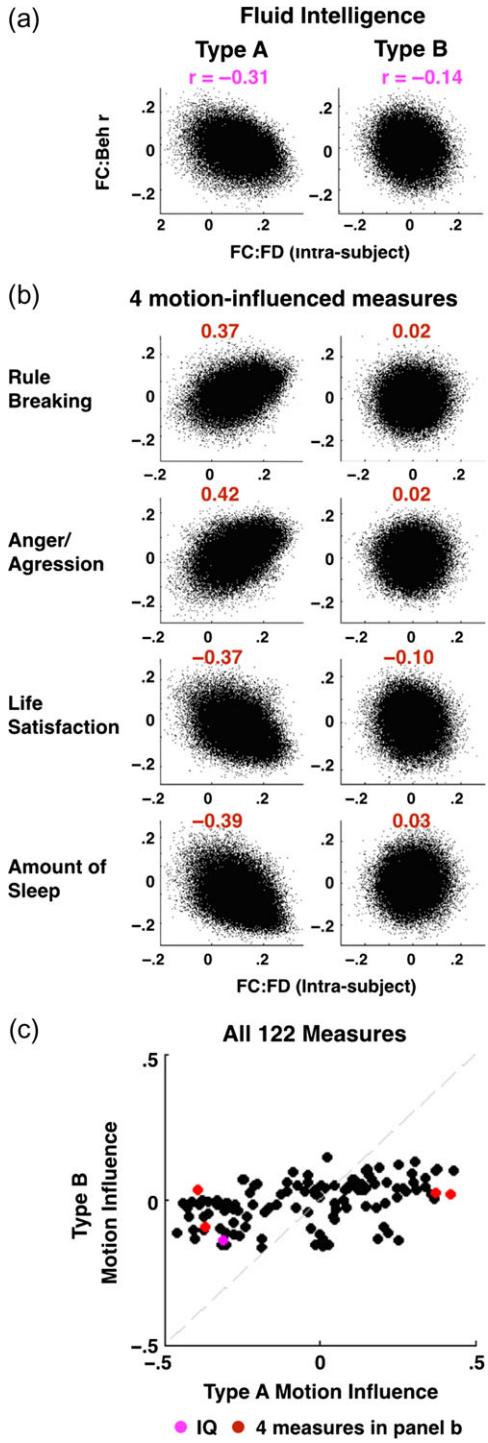

Figure 5. Type B processing reduced the influence of head motion across many behaviors. Each scatter plot shows FC:FD (intrasubject) weights versus FC: behavior (intersubject) correlations. A larger correlation suggests greater head motion influence (correlation coefficients greater than $r = 0.272$ are significant at $P > 0.05$ based on permutations). The left column is generated with Type A processing, the right column is generated with Type B processing. (*a*) The influence of head motion on FC:IQ relationships. *r*-Values are given above each plot. (*b*) The influence of head motion on FC:behavior relationships for 4 measures showing apparent influence of head motion but not included in Table 1. Pearson correlations are shown in red above each plot. (*c*) Across all 122 subject measures, the influence of head motion drops toward zero with additional cleaning steps included in Type B processing. IQ is shown in magenta and the 4 measures in Panel b are shown in red.

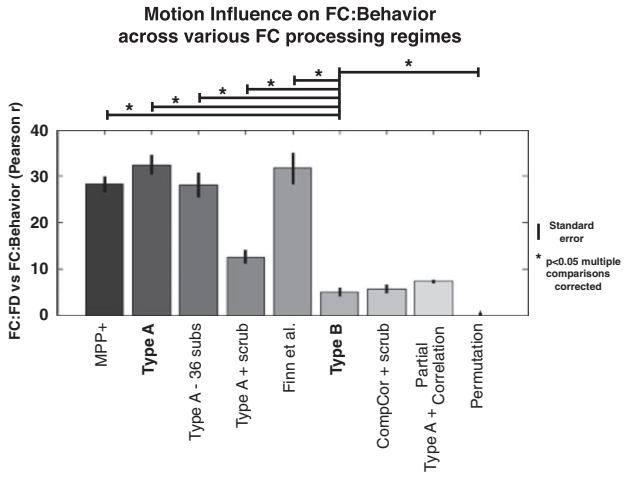

Figure 6. Motion influence on FC:IQ across FC processing regimes. The approach to estimate motion influence in Figure 3 was applied following several FC processing strategies. Bars indicate mean motion influence for the 19 behavior measures in table 1, error bars indicate standard error of the mean. Asterisks and horizontal bars above the indicate $P < 0.05$ following 8 two-tailed paired *t*-tests comparing Type B processing with all other processing regimes, Bonferroni corrected for multiple comparisons. "MPP+": HCP minimal preprocessing plus motion regression (24 regressors), demeaning, detrending, and variance normalization; "Type A–36 subs": 36 high-motion subjects were removed (matching those removed in Type A + scrub); Finn et al.: minimal preprocessing (excluding FIX), with regression of 24 motion parameters as well as mean gray, white, and ventricle time courses, and bandpass filtering (as used in Finn et al. 2015 prediction of IQ). CompCor + scrub: similar to Type B except CompCor regressors (10 white matter and ventricle PCA-derived regressors) were included and the gray matter regressor was excluded; Type A + partial correlation: "Permutation": the mean and SD of motion influence for 1000 random permutations of Type A processed FC data.

showed low motion influence (not significantly different from Type B). Importantly, Type B processing showed significantly greater motion influence than random permutations, indicating that some confounding influence is still present.

Discussion

We find that a large number of behavioral, demographic, and physiological measures (23 of 122) correlate with head motion in an fMRI scanner. Measures of cognitive ability, such as fluid intelligence, showed negative correlations; psychiatric scales (e.g., DSM Antisocial Behavior), tobacco use, and BMI showed positive correlations (Table 1). This is consistent with a prior report linking measures of impulsivity to head motion (Kong et al. 2014). The particularly strong correlation between BMI and FD (Figure S5) may be mediated in part by respiratory effort, as can be inferred from respiratory oscillations in FD time courses (Fig. S2). Larger individuals typically breathe more rapidly and with greater effort in the supine position, thereby generating respiration-related motion artifact.

For behavioral measures that correlated with head motion, we observed correlation between intrasubject FC:FD topography and FC:behavior topography (Fig. 3*a*/*b*). Theoretically, correlations between head motion and FC could be mediated by true neurobiological differences between movers and nonmovers (Zeng et al. 2014). However, this line of reasoning cannot explain FC:FD relationships evaluated on the basis of intrasubject effects of motion (Fig. 2).

To determine if previously published data cleaning steps can reduce the influence of head motion on FC:behavior

correlations, we introduced Type B processing. Type B processing includes multiple time course regression, bandpass filtering, scrubbing of high-motion and high variance frames, and total exclusion of high-motion fMRI sessions (Fig. 1). Type B processing substantially altered the topography of FC:IQ correlations and significantly reduced the influence of head motion (Figs. 3 and 5). These results suggest that FC:behavior relationships of the type illustrated in Figure 3*a* are largely attributable to factors other than IQ.

In a final analysis, we compared 8 different data processing regimes and found that 2 approaches reduced motion influence at levels comparable to Type B: 1) Type B processing excluding an explicit global signal regressor but using additional PCA-based nuisance regressors (CompCor) and 2) Type A processing followed by partial correlation (rather than full Pearson correlation). A prior study by Muschelli et al. found that some distance-related motion artifact persisted following CompCor regression, but was removed when scrubbing was performed in addition to CompCor (Muschelli et al. 2014). Thus, we included scrubbing in our CompCor processing regime, and found it to be effective at reducing motion influence. Our results suggest that alternative approaches that do not employ gray matter signal regression per-se may be equally effective at reducing motion influence.

As there is no reason to believe that the influence of head motion on FC:behavior relationships is specific to HCP data, our results imply that many previously published results identifying R-fMRI differences across or between groups should be critically re-examined. Autism spectrum disorder provides a cautionary tale of this imperative. Early R-fMRI studies of ASD identified numerous FC abnormalities, primarily, reduced correlations (Cherkassky et al. 2006; Monk et al. 2009; Jones et al. 2010). However, as additional reports accumulated, substantial inconsistencies across studies became apparent. These inconsistencies were attributed to interlaboratory variability in methodology (Müller et al. 2011). As approaches for removing motion artifact became more widely recognized, several papers incorporating appropriate controls for head motion reported largely typical findings in high functioning adults with ASD (Redcay et al. 2013; Tyszka et al. 2014; Mitra et al. 2015).

Despite good faith efforts to account for head motion in prior studies, our findings suggest that complete removal of the confounding influence of head motion is difficult or impossible (Fig. 5). Nevertheless, when a sufficient amount of R-fMRI data has been acquired, data sets corrupted by motion may remain largely viable after adequate steps have been taken to remove artifactual variance. In our Type B processing, only 36 subjects were removed from the cohort of 461 (23 out of 284 for reconstruction version 2). Additional maneuvers for reducing the impact of head motion would be to balance head motion across groups and to use individual FD measures as nuisance regressor at the group level, with the caveats pointed out by Power et al. (2014).

Limitations

Head motion, inferred from retrospective image realignment, may be linked to BOLD signal artifacts through several mechanisms. Most obviously, head motion leads to spin history effects that generate artifacts on the basis of imaging physics (Friston et al. 1996). However, head motion very likely is linked to physiological modulators of the BOLD signal. In particular, changes in respiratory rate occurring spontaneously or in association with sighs, coughs, etc., may induce large nonneural transients in the BOLD signal through changes in arterial pCO_2 (Wise et al. 2004). Respiratory rate modulations also potentially affect the BOLD signal through changes in cerebral perfusion consequent to fluctuating cardiac rate (Raj et al. 2001; Birn 2012). Finally, as discussed, some modulations of the BOLD signal associated with head motion may reflect true sensory or motor neural responses (Yan et al. 2013; Zeng et al. 2014). Thus, observed head motion may ultimately represent a proxy for a variety of artifactual as well as neural transients in the BOLD signal.

Head motion is one of the multiple physiological confounds with known or not fully understood influence on the BOLD signal (Raj et al. 2001; Shmueli et al. 2007; Birn 2012). Techniques have been developed to reduce cardio-pulmonary pulsation artifacts in R-fMRI data using pulse oximeter and respiratory belt records (Chang and Glover 2009; Murphy et al. 2013). At the time of this study, these records were not available. However, pulse oximeter and respiratory belt data were acquired by the HCP and should be accessible in later releases.

Moreover, an approach that defines nuisance regressors on the basis of voxels with high temporal SD (tCompCor) was previously found to be equal or more effective than anatomical CompCor (CSF and white matter) (Behzadi et al. 2007). The benefit of such an approach on HCP data preprocessed using FIX remains to be determined.

Interpreting Observed FC:Behavior Relationships

The persistent influence of head motion (Fig. 5) suggests that, even after data cleaning, the interpretation of FC:behavior correlations must be approached with caution. FC within a broad topography may directly relate to IQ (Cole et al. 2013; Finn et al. 2015; Smith et al. 2015), with the inference that IQ also mediates physiological factors as well as propensity to move. The difficulty with this interpretation is that motion imposes a stereotypical FC topography in R-fMRI data (Yan et al. 2013). In fact, this "motion artifact topography" is the same set of regions within which FC seems to predict IQ (cf. Fig. 3*a* to Finn et al. 2015). An alternative interpretation is that there is a relation between IQ and other factors (such as head motion) that influence FC. Thus, FC:IQ correlations may be observed that do not represent true neural correlates of intelligence. Therefore, on the basis of correlations alone, it is not possible to elucidate the true causal structure underlying physical factors, head motion, IQ, and FC.

This uncertainty points to a larger challenge in the interpretation of observed FC:behavior relationships. Specifically, it is essential to avoid over interpreting an observed correlation between variables. Just as we would hesitate to ascribe a causal link between years of education and head motion (shown to be correlated in Table 1), so should we be careful when interpreting a correlation between FC and IQ. There is a long history of attempting to correlate variability in various brain measures to behavior; for the most part, causal inferences derived from these studies have not stood the test of time (Gould 1996). Therefore, it is essential to emphasize that properties of the brain inferred on the basis of BOLD fMRI FC remain uncertain, and a neurobiologically meaningful basis for interindividual differences in FC remains to be established. It is only by combing technical improvements in the acquisition and analysis of R-fMRI data with careful investigation of FC:behavior relationships that we can begin to understand how behavioral measures relate to neural function.

Glossary

- BOLD – blood oxygenation level dependent
- DVARS – signal variance across the whole brain
- EPI – echo-planar imaging
- FC – Functional connectivity
- FC:Behavior – correlation between FC and behavior
- FD – framewise displacement (head motion)
- FIR filter – finite impulse response filter
- FIX-ICA – FMRIB's ICA-based X-noiseifier using independent component analysis
- HCP – Human Connectome Project
- IQ – fluid intelligence score on Penn progressive matrices
- MPP – minimal preprocessing pipeline
- MTR – multiple timecourse regression
- PCA – principal components analysis
- R-fMRI – resting state functional magnetic resonance imaging
- DVARS – signal variance across the whole brain
- IQ – score on Penn progressive matrices (fluid intelligence)

Supplementary Material

Supplementary material can be found at: http://www.cercor.xfordjournals.org.

Funding

National Institute of Child Health and Human Development award (5R01HD061117 to M.C.); National Institute of Child Health and Human Development (U54 HD087011 to A.Z.S.); American Heart Association Predoctoral Fellowship Award (14PRE19610010 to J.S.S.).

Notes

The authors thank Jonathan Power, Tomer Livne, Greg Burgess, Matthew Glasser, Deanna Barch, and David Van Essen for helpful comments and discussion. *Conflict of Interest*: None declared.

References

Andrews-Hanna JR, Snyder AZ, Vincent JL, Lustig C, Head D, Raichle ME, Buckner RL. 2007. Disruption of large-scale brain systems in advanced aging. Neuron. 56:924–935.

Barkhof F, Haller S, Rombouts SARB. 2014. Resting-state functional MR imaging: a new window to the brain. Radiology. 272:29–49.

Behzadi Y, Restom K, Liau J, Liu TT. 2007. A component based noise correction method (CompCor) for BOLD and perfusion based fMRI. NeuroImage. 37:90–101.

Birn RM. 2012. The role of physiological noise in resting-state functional connectivity. NeuroImage. 62:864–870.

Carp J. 2013. Optimizing the order of operations for movement scrubbing: Comment on Power et al. NeuroImage. 76:436–438.

Chai XJ, Ofen N, Gabrieli JDE, Whitfield-Gabrieli S. 2013. Selective development of anticorrelated networks in the intrinsic functional organization of the human brain. J Cogn Neurosci. 26:501–513.

Chang C, Glover GH. 2009. Relationship between respiration, end-tidal CO2, and BOLD signals in resting-state fMRI. NeuroImage. 47:1381–1393.

Cherkassky VL, Kana RK, Keller TA, Just MA. 2006. Functional connectivity in a baseline resting-state network in autism. Neuroreport. 17:1687–1690.

Cole MW, Reynolds JR, Power JD, Repovs G, Anticevic A, Braver TS. 2013. Multi-task connectivity reveals flexible hubs for adaptive task control. Nat Neurosci. 16:1348–1355.

Deen B, Pelphrey K. 2012. Perspective: brain scans need a rethink. Nature. 491:S20.

Dosenbach NUF, Nardos B, Cohen AL, Fair DA, Power JD, Church JA, Nelson SM, Wig GS, Vogel AC, Lessov-Schlaggar CN, et al. 2010. Prediction of individual brain maturity using fMRI. Science. 329:1358–1361.

Fair DA, Dosenbach NUF, Church JA, Cohen AL, Brahmbhatt S, Miezin FM, Barch DM, Raichle ME, Petersen SE, Schlaggar BL. 2007. Development of distinct control networks through segregation and integration. Proc Natl Acad Sci. 104:13507–13512.

Fair DA, Nigg JT, Iyer S, Bathula D, Mills KL, Dosenbach NUF, Schlaggar BL, Mennes M, Gutman D, Bangaru S, et al. 2013. Distinct neural signatures detected for ADHD subtypes after controlling for micro-movements in resting state functional connectivity MRI data. Front Syst Neurosci. 6:80.

Finn ES, Shen X, Scheinost D, Rosenberg MD, Huang J, Chun MM, Papademetris X, Constable RT. 2015. Functional connectome fingerprinting: identifying individuals using patterns of brain connectivity. Nat Neurosci. 18:1664–1671.

Fornito A, Bullmore ET. 2015. Connectomics: a new paradigm for understanding brain disease. Eur Neuropsychopharmacol. 25:733–748.

Friston KJ, Williams S, Howard R, Frackowiak RSJ, Turner R. 1996. Movement-related effects in fMRI time-series. Magn Reson Med. 35:346–355.

Gordon EM, Laumann TO, Adeyemo B, Huckins JF, Kelley WM, Petersen SE. 2016. Generation and evaluation of a cortical area parcellation from resting-state correlations. Cereb Cortex. 26:288–303.

Glasser MF, Sotiropoulos SN, Wilson JA, Coalson TS, Fischl B, Andersson JL, Xu J, Jbabdi S, Webster M, Polimeni JR, Van Essen DC, Jenkinson M. 2013. The minimal preprocessing pipelines for the Human Connectome Project. NeuroImage. 80:105–124.

Gould SJ. 1996. The Mismeasure of Man. W. W. Norton & Company, New York, NY.

Jo HJ, Saad ZS, Simmons WK, Milbury LA, Cox RW. 2010. Mapping sources of correlation in resting state FMRI, with artifact detection and removal. NeuroImage. 52:571–582.

Jones TB, Bandettini PA, Kenworthy L, Case LK, Milleville SC, Martin A, Birn RM. 2010. Sources of group differences in functional connectivity: an investigation applied to autism spectrum disorder. NeuroImage. 49:401–414.

Kong X, Zhen Z, Li X, Lu H, Wang R, Liu L, He Y, Zang Y, Liu J. 2014. Individual differences in impulsivity predict head motion during magnetic resonance imaging. PLOS One. 9:e104989.

Liu Y, Yu C, Zhang X, Liu J, Duan Y, Alexander-Bloch AF, Liu B, Jiang T, Bullmore E. 2014. Impaired long distance functional connectivity and weighted network architecture in Alzheimer's disease. Cereb Cortex. 24:1422–1435.

Mitra A, Snyder AZ, Constantino JN, Raichle ME. 2015. The lag structure of intrinsic activity is focally altered in high functioning adults with autism. Cereb Cortex. bhv294.

Monk CS, Peltier SJ, Wiggins JL, Weng S-J, Carrasco M, Risi S, Lord C. 2009. Abnormalities of intrinsic functional connectivity in autism spectrum disorders. NeuroImage. 47:764–772.

Müller R-A, Shih P, Keehn B, Deyoe JR, Leyden KM, Shukla DK. 2011. Underconnected, but How? A survey of functional connectivity MRI studies in autism spectrum disorders. Cereb Cortex. 21:2233–2243.

Murphy K, Birn RM, Bandettini PA. 2013. Resting-state fMRI confounds and cleanup. NeuroImage, Mapping the Connectome. 80:349–359.

Muschelli J, Nebel MB, Caffo BS, Barber AD, Pekar JJ, Mostofsky SH. 2014. Reduction of motion-related artifacts in resting state fMRI using a CompCor. NeuroImage. 96:22–35.

Power JD, Barnes KA, Snyder AZ, Schlaggar BL, Petersen SE. 2012. Spurious but systematic correlations in functional connectivity MRI networks arise from subject motion. NeuroImage. 59:2142–2154.

Power JD, Schlaggar BL, Petersen SE. 2015. Recent progress and outstanding issues in motion correction in resting state fMRI. NeuroImage. 105:536–551.

Raj D, Anderson AW, Gore JC. 2001. Respiratory effects in human functional magnetic resonance imaging due to bulk susceptibility changes. Phys Med Biol. 46:3331.

Redcay E, Moran JM, Mavros PL, Tager-Flusberg H, Gabrieli JDE, Whitfield-Gabrieli S. 2013. Intrinsic functional network organization in high-functioning adolescents with autism spectrum disorder. Front Hum Neurosci. 7:573.

Salimi-Khorshidi G, Douaud G, Beckmann CF, Glasser MF, Griffanti L, Smith SM. 2014. Automatic denoising of functional MRI data: combining independent component analysis and hierarchical fusion of classifiers. NeuroImage. 90:449–468.

Satterthwaite TD, Wolf DH, Loughead J, Ruparel K, Elliott MA, Hakonarson H, Gur RC, Gur RE. 2012. Impact of in-scanner head motion on multiple measures of functional connectivity: relevance for studies of neurodevelopment in youth. NeuroImage. 60:623–632.

Shirer WR, Jiang H, Price CM, Ng B, Greicius MD. 2015. Optimization of rs-fMRI pre-processing for enhanced signal-noise separation, test-retest reliability, and group discrimination. NeuroImage. 117:67–79.

Shmueli K, van Gelderen P, de Zwart JA, Horovitz SG, Fukunaga M, Jansma JM, Duyn JH. 2007. Low-frequency fluctuations in the cardiac rate as a source of variance in the resting-state fMRI BOLD signal. NeuroImage. 38:306–320.

Siegel JS, Power JD, Dubis JW, Vogel AC, Church JA, Schlaggar BL, Petersen SE. 2014. Statistical improvements in functional magnetic resonance imaging analyses produced by censoring high-motion data points. Hum Brain Mapp. 35:1981–1996.

Smith SM, Beckmann CF, Andersson J, Auerbach EJ, Bijsterbosch J, Douaud G, Duff E, Feinberg DA, Griffanti L, Harms MP, et al. 2013. Resting-state fMRI in the human connectome project. NeuroImage. 80:144–168.

Smith SM, Miller KL, Salimi-Khorshidi G, Webster M, Beckmann CF, Nichols TE, Ramsey JD, Woolrich MW. 2011. Network modelling methods for FMRI. NeuroImage. 54:875–891.

Smith SM, Nichols TE, Vidaurre D, Winkler AM, Behrens TEJ, Glasser MF, Ugurbil K, Barch DM, Van Essen DC, Miller KL. 2015. A positive-negative mode of population covariation links brain connectivity, demographics and behavior. Nat Neurosci. 18:1565–1567.

Smyser CD, Inder TE, Shimony JS, Hill JE, Degnan AJ, Snyder AZ, Neil JJ. 2010. Longitudinal analysis of neural network development in preterm infants. Cereb Cortex. 20: 2852–2862.

Snyder AZ, Raichle ME. 2012. A brief history of the resting state: the Washington university perspective. NeuroImage. 62: 902–910.

Tyszka JM, Kennedy DP, Paul LK, Adolphs R. 2014. Largely typical patterns of resting-state functional connectivity in high-functioning adults with autism. Cereb Cortex. 24: 1894–1905.

Uğurbil K, Xu J, Auerbach EJ, Moeller S, Vu AT, Duarte-Carvajalino JM, Lenglet C, Wu X, Schmitter S, Van de Moortele PF, et al. 2013. Pushing spatial and temporal resolution for functional and diffusion MRI in the Human Connectome Project. NeuroImage. 80:80–104.

Van Dijk KRA, Sabuncu MR, Buckner RL. 2012. The influence of head motion on intrinsic functional connectivity MRI. NeuroImage. 59:431–438.

van Eimeren T, Monchi O, Ballanger B, Strafella AP. 2009. Dysfunction of the default mode network in Parkinson disease: a functional magnetic resonance imaging study. Arch Neurol. 66:877–883.

Van Essen DC, Smith SM, Barch DM, Behrens TEJ, Yacoub E, Ugurbil K. 2013. The WU-Minn Human Connectome Project: an overview. NeuroImage. 80:62–79.

Wise RG, Ide K, Poulin MJ, Tracey I. 2004. Resting fluctuations in arterial carbon dioxide induce significant low frequency variations in BOLD signal. NeuroImage. 21:1652–1664.

Yan C-G, Cheung B, Kelly C, Colcombe S, Craddock RC, Di Martino A, Li Q, Zuo X-N, Castellanos FX, Milham MP. 2013. A comprehensive assessment of regional variation in the impact of head micromovements on functional connectomics. NeuroImage. 76:183–201.

Zeng L-L, Wang D, Fox MD, Sabuncu M, Hu D, Ge M, Buckner RL, Liu H. 2014. Neurobiological basis of head motion in brain imaging. Proc Natl Acad Sci. 111:6058–6062.